DAΦNE TECHNICAL NOTE

INFN - LNF, Accelerator Division

Frascati, November 18, 1996

Note: **G-43**

POWER LOSSES IN THE DAΦNE BELLOWS SHIELDS

G.O. Delle Monache, A. Gallo, F. Marcellini, M. Zobov

1. Introduction

Two kinds of DAΦNE RF shielded bellows have been designed. A special design effort has been made to avoid using sliding contacts in the shields[1] since their reliability is quite poor at very intensive current, as pointed out by the experience of existing machines.

Bellows of the first kind are those placed between the arcs and the straight sections; they have to compensate for 35 mm of vacuum chamber free expansion and 10 mm of horizontal offset during the bake-out. Due to their considerable length (≈ 220 mm) we call them "long bellows".

There are 8 such bellows per ring: 4 of them, being located downstream the arcs, have a lateral slot in the shield to let the synchrotron radiation be absorbed on the outer chamber.

Bellows of the second kind are those placed in the various machine straight sections. There are 20 such bellows per ring, and in spite of the different chamber cross sections, they are basically made in the same way, being 45 mm long and allowing an expansion of 10 mm. For this reason we call them "short bellows".

The aim of this note is to estimate the power dissipation in the bellows shields coming from different sources (Joule losses, resonant coupling to the beam, synchrotron radiation hitting) as a base for a thermal stress analysis of the structures themselves.

2. Short Bellows

A picture of a DAΦNE short bellows is shown in Fig. 1. In order to prevent e.m. coupling between the beam and the bellows outer chamber, following a suggestion of A. Ghigo, a number of small bellows (Ø=7.9 mm) spaced at 1 mm has been placed to short circuit the bellows gap, following with good approximation the shape of the chamber cross section. The mini-bellows are produced by electro-deposition of ≈ 30 μm thickness pure copper.

There are two kinds of short bellows: the first one fits the shape of a rectangular (54 x 88 mm) chamber with 32 mini bellows, while the second one fits the shape of a pseudo-elliptical (120 x 200 mm) chamber with 60 mini bellows. In the following we will deal with the power loss estimate of the first kind of short bellows since, having a lower number of shielding elements, it is certainly more prone to thermal stress.

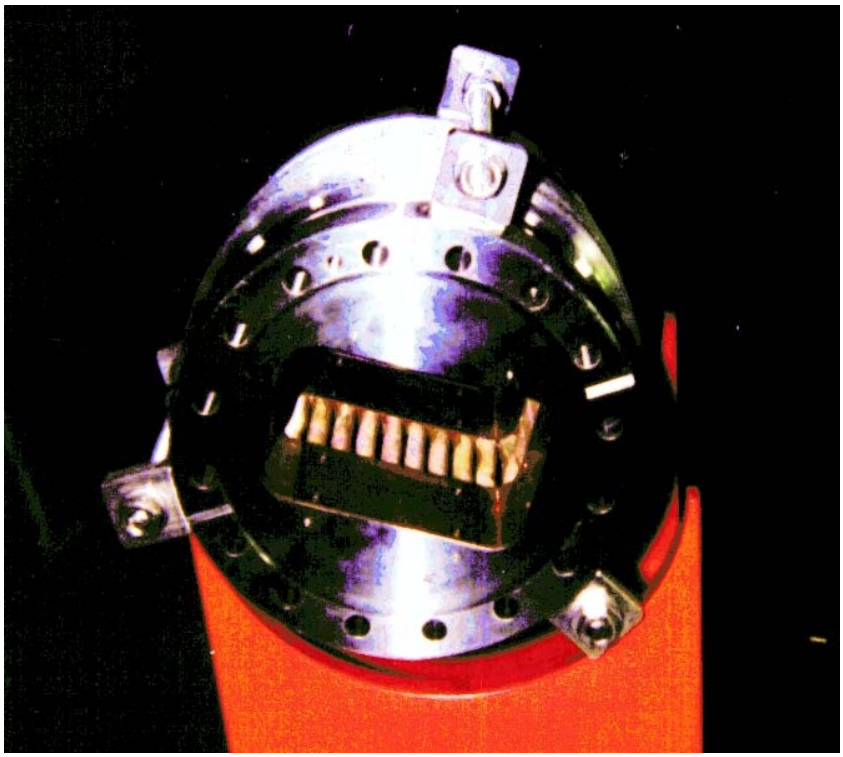

Figure 1: Picture of the shielded short bellows

A wire measurement of a short bellows impedance on a prototype is shown in Fig. 2. Since there is no significant difference between the bellows and a reference tube frequency response up to 3.5 GHz, we can conclude that this kind of structure does not contain longitudinal resonances which could drive coupled bunch instability or produce bellows overheating while interacting with the bunched beam.

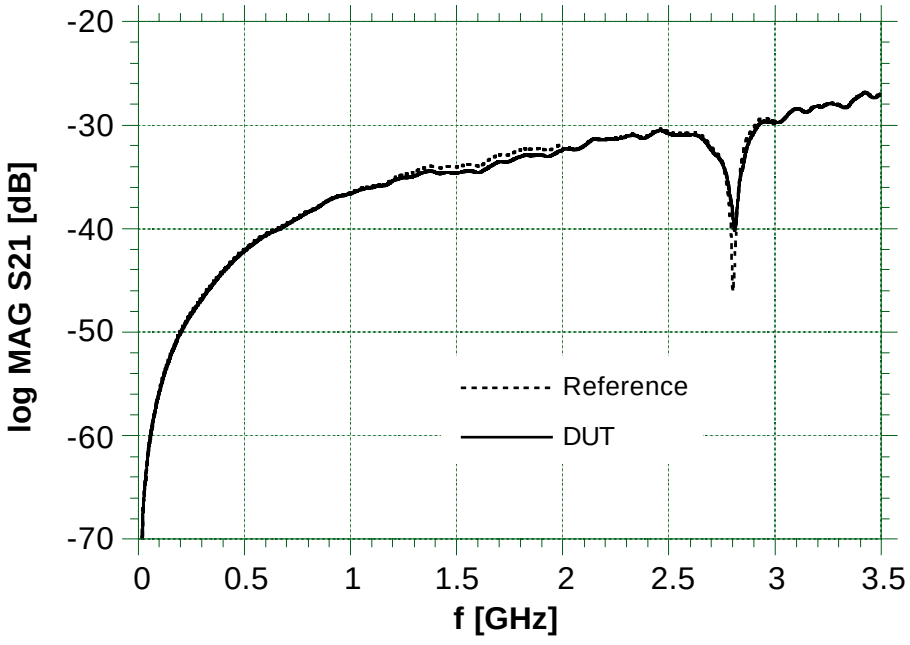

Figure 2: Short bellows impedance wire measurement (with reference)

2.1 Joule Losses

Being a longitudinal mode free structure, the short bellows e.m. interaction with the beam is limited to Joule dissipation produced by the beam image currents in the shielding elements.
To compute the current flow through any mini-bellows we have considered the image current distribution on the rectangular chamber excited by the current flowing on an inner round conductor placed on the chamber axis. The normalized current distribution, i.e. the tangential magnetic field H_t divided by the exciting current as given by the HFSS code[2], is shown in Fig. 3. The overall current flow in each mini bellows can be computed by discretizing the current density. It comes out that the closest shielding element with respect to the beam axis is the most stressed one, and it shunts about 8.2 % of the total beam current.

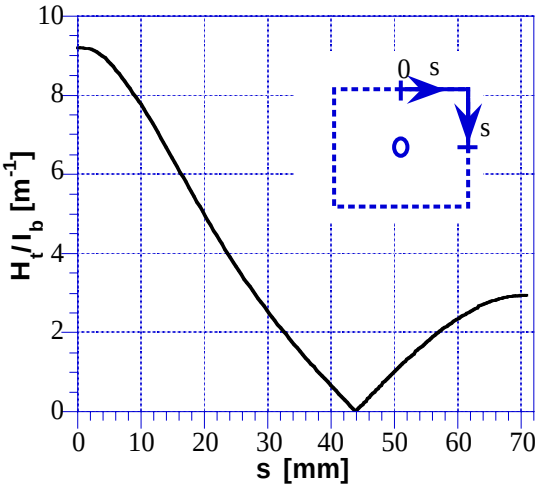

Figure 3: Field distribution along the rect wg contour.

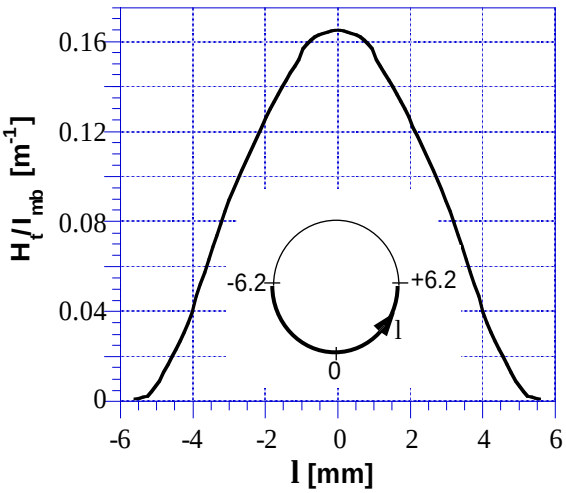

Figure 4: Field distribution along the mini-bellows contour.

In order to compute the power dissipation, the current distribution along the mini-bellows cross-section contour must be known. To calculate it, we carried out a computer simulation based on the same code considering plain cylinders instead of mini-bellows. The normalized current distribution along the cylinder contour is shown in Fig. 4, where $\boldsymbol{H_t}$ is the tangential magnetic field and $\boldsymbol{I_{mb}}$ the total image current flowing along the mini-bellows. The power dissipation is therefore given by:

$$P_d = \frac{1}{2} A \sum_n R_S(nf_0)\, I_n^2 \qquad (1)$$

where f_0 is the bunch repetition frequency, R_s is the copper surface resistivity, I_n are the bunch spectrum amplitudes (including the roll-off factor due to the finite bunch length) and A is a dimensionless form factor given by:

$$A = l_z \int_{\substack{bellows\\contour}} \left(H_t / I_b\right)^2 dl \qquad (2)$$

where l_z is the mini-bellows total length. Considering a 5 Amps beam current distributed over 120 bunches of 3 cm length, eq. 1 gives a Joule loss of ≈ 200 mW on the most stressed mini-bellows.

2.2 Synchrotron radiation interception

Although the short-bellows are placed in the straight sections quite far from the bending magnets, there is still a certain amount of synchrotron radiation intercepted by the shielding elements laying close to the machine horizontal plane on the outward side. In the 120 bunches, 5 Amps case the estimated power associated to synchrotron radiation entering the bellows is ≈ 500 mW[3]. Since there are two mini-bellows placed symmetrically with respect to the horizontal plane and separated by 1 mm, the power dissipation on each one is at most 250 mW. Anyway, part of synchrotron radiation passes through the 1 mm mini-bellows separation and is dissipated on the bellows outer chamber, and therefore 250 mW is a conservative figure.

The contribution of the Joule losses for those mini-bellows placed near the horizontal plane can be worked out from the plot of Fig. 3 and is ≈20 mW, a negligible amount with respect to the dissipation coming from synchrotron radiation.

2.3 Thermal analysis

From the above considerations it turns out that the most stressed shielding mini-bellows are those placed outward nearby the horizontal plane (≈ 270 mW mostly coming from synchrotron radiation) and those placed nearby the longitudinal vertical plane (≈ 200 mW entirely coming from Joule dissipation).

The good thermal conductivity of copper allows us to consider the power as uniformly distributed on the mini bellows contour in the thermal analysis, although this is not actually the case. On this basis, the maximum temperature rise can be evaluated applying the following formula:

$$T_{Max} - T_0 = \frac{ql}{8\,\pi dh\lambda} \qquad (3)$$

which is a monodimensional solution of the Poisson equation for the heat propagation. Here q[W] is the dissipated power, l[m] is the mini bellows surface length, d[m] the mini bellows diameter, h[m] the thickness of copper deposition and λ[W/m°K] the thermal conduction coefficient (350÷400 for copper).

The results show that there is a longitudinal temperature gradient along the mini-bellows, with the hottest point located in the center, reaching ≈61°C in the case of 270 mW dissipation, and ≈ 50 °C in the case of 200 mW dissipation, assuming an environment temperature of 20 °C.

3. Long Bellows.

A sketch of a DAΦNE long bellows is shown in Fig. 5. The bellows outer chamber is shielded by a number of vertical waved strips of 12 mm height and 0.15 mm thickness reproducing the shape of the rectangular 53 x 86 mm vacuum chamber. The strips are pre-formed in the waved shape and are made of a Cu-Be alloy (C17500) to guarantee high elasticity and good thermal and electrical conductivities.

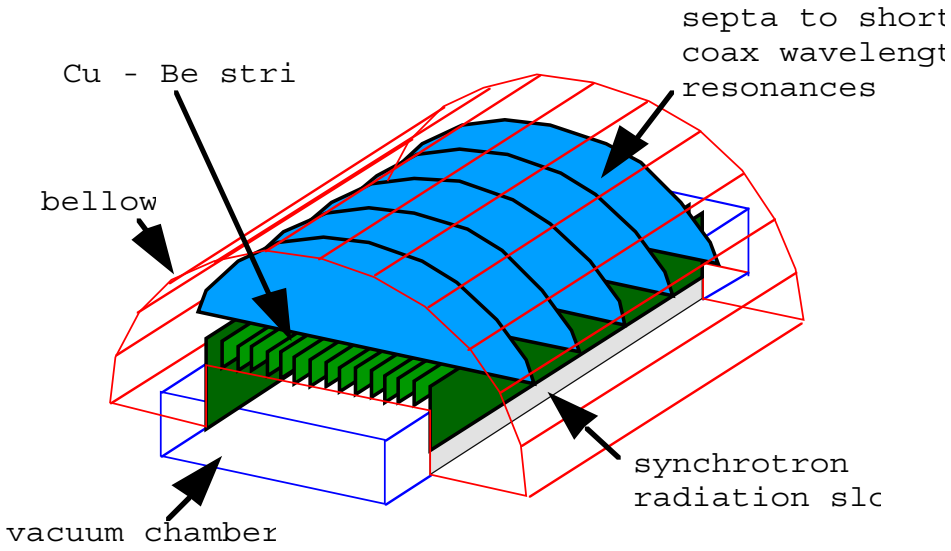

Figure 5: Sketch of a shielded long bellows

The side strips are higher in order to reproduce the lateral chamber wall, but at least one slot has to be left on the outward shield surface of the bellows placed downstream the beam, in order to let the large amount of synchrotron radiation energy get out and be dissipated on the bellows outer chamber. Unfortunately, this slot is responsible for coupling between the beam and the pseudo-coaxial resonator having the shield as the inner conductor and the bellows chamber as the external one, so that the beam coupling impedance of the device exhibits some resonances of the $n\lambda/2$ type.

In order to weaken and reduce the number of these resonances, transversal connections ("combs") and e.m. wave scrapers ("septa") have been applied to the strips, as shown in Fig. 5. Combs and septa shorten the effective electrical length of $n\lambda/2$ resonances, so that strong modes can only appear at rather high frequency (≥ 2.5 GHz) where the beam power spectrum falls rapidly.

3.1 Resonant losses

A wire measurement of a long bellows prototype impedance up to 3.5 GHz with a side slot on one or both sides has been carried out. A Ø 3 mm copper wire has been introduced in the bellows, while ferrite tiles have been inserted inside the beam chamber closing flanges of the device in order to prevent beam tube resonances which can affect the measurement.

The list of the measured modes in the case of a single side slot is reported in Table I. The peak coupling impedances are of the order of 1 Ω below 2.5 GHz and reach some tens of Ω's above that frequency, while the impedance values weighted by the 3 cm bunch roll-off factor do not exceed few Ωs. The Q values are of the order of few hundreds. The power delivered to the bellows originated by resonant coupling with the beam spectrum lines is given by:

$$P_{res} = 2 * I_b^2 \sum_{\substack{k=all\\modes}} \sum_{\substack{n=all\\beam\ lines}} \frac{(Z_k)_{roll-off}}{1 + Q_k^2 \left(nf_0 / f_k - f_k / nf_0 \right)^2} \qquad (4)$$

where $(Z_k)_{roll-off}$, Q_k and f_k are the mode parameters and I_b is the dc value of the beam current.

Table I

f [MHz]	Q	Z [Ω]	$Z_{roll\text{-}off}$ [Ω]	f/f_0	P_{res_k} [W]
983.759	550.000	3.55000	2.42270	2.6709	0.0073828
1270.490	287.000	2.87000	1.51750	3.4494	0.0117400
1550.350	1020.000	0.81700	0.31632	4.2092	0.0014603
1664.040	668.000	3.13000	1.04900	4.5179	0.0028490
1905.170	673.000	0.96400	0.23002	5.1726	0.0055066
1960.150	623.000	1.23000	0.26987	5.3219	0.0006012
2183.160	292.000	3.13000	0.47684	5.9273	0.4618200
2271.860	884.000	1.78000	0.23200	6.1682	0.0048526
2381.190	490.000	8.87000	0.94576	6.4650	0.0088195
2451.770	516.000	2.76000	0.25720	6.6566	0.0047677
2564.840	250.000	31.30000	2.33160	6.9636	14.9690000
2631.060	338.000	1.48000	0.09624	7.1434	0.0254660
2782.860	210.000	15.33000	0.72071	7.5555	0.0623500
2871.560	668.000	1.08000	0.04165	7.7964	0.0017534
3027.740	518.000	13.70000	0.36726	8.2204	0.0231280
3180.790	726.000	6.02000	0.11090	8.6359	0.0015413
3255.120	592.000	3.02000	0.04606	8.8378	0.0049527
3281.360	285.000	40.25000	0.57369	8.9090	0.8299600

P_{res}≈16.43 W

The amount of power delivered by the beam to the resonant modes, given by eq. 4), is extremely sensitive to the mode resonant frequencies with respect to the beam spectrum exciting lines, which are very difficult to determine. In fact the wire method always perturbs the frequencies to a certain extent. Moreover, the measurements show that the mode frequencies are also sensitive to the compression status of the bellows, which is likely to be different on bench with respect to the operating regime.

If the mode frequencies were actually those reported in Table I, the total amount of dissipated power would be $\boldsymbol{P}_{res} \approx 16.5$ W. On the other hand, it is worth establishing whether this is a conservative figure or not. As shown in the appendix, if we assume that the modes of Table I can freely spread over the frequency span between two beam spectrum lines, we can evaluate the probability that the dissipated power is lower than any given value. This is equivalent to the assumption that the actual frequency location of the modes is completely unknown, while the impedance and the Q values are those given by the wire measurement.

The result is the probability function $p_T(\boldsymbol{P})$ plot in Fig. 6, representing the probability that the dissipated power is lower than $\boldsymbol{P}$. The probability function at $\boldsymbol{P}$≈16.5 W is ≈76%, while the 50% point corresponds to ≈5 W. This indicates that a resonant loss contribution of 16.5 W to the total power dissipation in the long bellows can be considered as a conservative enough estimate.

Another issue is to establish how this power is distributed inside the device. As already stated, from code simulations (MAFIA[4], HFSS) it is evident that the modes coupled to the beam are $n\lambda/2$ TEM resonances of a pseudo-coaxial line. The series loss resistance r_{loss} of a coaxial line is proportional to:

$$r_{loss} \propto \frac{R_{S_{in}}}{\varnothing_{in}} + \frac{R_{S_{out}}}{\varnothing_{out}} \tag{5}$$

where $\varnothing_{in}, \varnothing_{out}$ and $R_{S_{in}}, R_{S_{out}}$ are respectively the inner and outer diameters and surface resistivities. Therefore the power share between inner and outer conductor is given by:

$$\frac{P_{in}}{P_{out}} = \frac{\varnothing_{out}}{\varnothing_{in}} \frac{R_{S_{in}}}{R_{S_{out}}} = \frac{\varnothing_{out}}{\varnothing_{in}} \sqrt{\frac{\sigma_{out}}{\sigma_{in}}} \tag{6}$$

where $\sigma_{in}, \sigma_{out}$ are the inner and outer electrical conductivities. In our case the ratio between the equivalent diameter of the outer conductor (the bellows chamber) and the inner conductor (the shield) is ≈1.5, while the ratio between the outer (made of stainless steel) and inner (made of Cu-Be alloy) conductivities is ≈.033, so that the power ratio between inner and outer comes out to be ≈.27. This means that only ≈ 3.5 out of 16.5 W are dissipated on the shield and may contribute to the structure overheating, while the remaining 13 W are dissipated on the outer chamber, which is in thermal contact with air at room temperature.

Furthermore, taking into account the field distribution of the TEM resonances, we can assume that the power dissipated on the shield is uniformly distributed. This means that the resonant loss on the side strips, which are the widest, is ≈420 mW each, while on the other strips the dissipation is limited to ≈65 mW. These data are the basis for the thermal analysis.

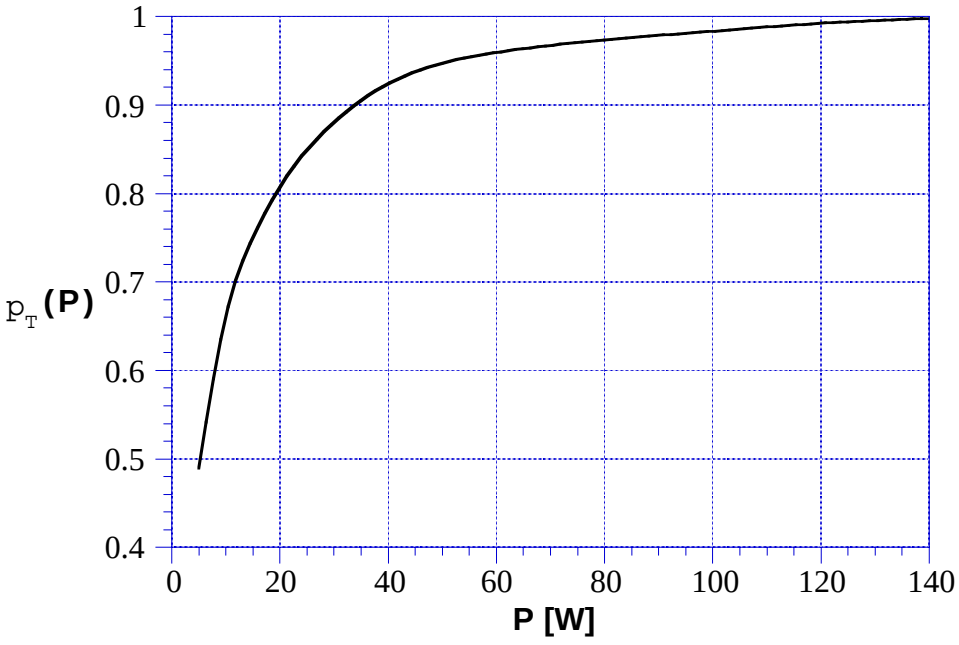

Figure 6: Total probability function.

3.2 Joule Losses

In addition to the resonant losses in the long bellows, we have to consider the Joule dissipation produced by the beam image current in the strips as in the already described case of the short bellows.

To compute the current flow through any strip we have considered again the current distribution on the rectangular chamber which is very much similar to that of Fig. 3. The overall current flow in each strip can be computed by discretizing the current density. The result is that among the 12 mm wide strips, those shunting the largest amount (≈5.1% each) of the total image current are placed near the vertical symmetry plane, while the wider lateral strips shunt ≈6.4 % of the image current each.

The power can be computed again according to eqs. (1) and (2), where the form factor $\boldsymbol{A}$ in this case is the integral along the strip contour of the square of the current distribution shown in Fig. 7, normalized to the strip current $\boldsymbol{I_s}$ and obtained again by means of a dedicated HFSS code simulation.

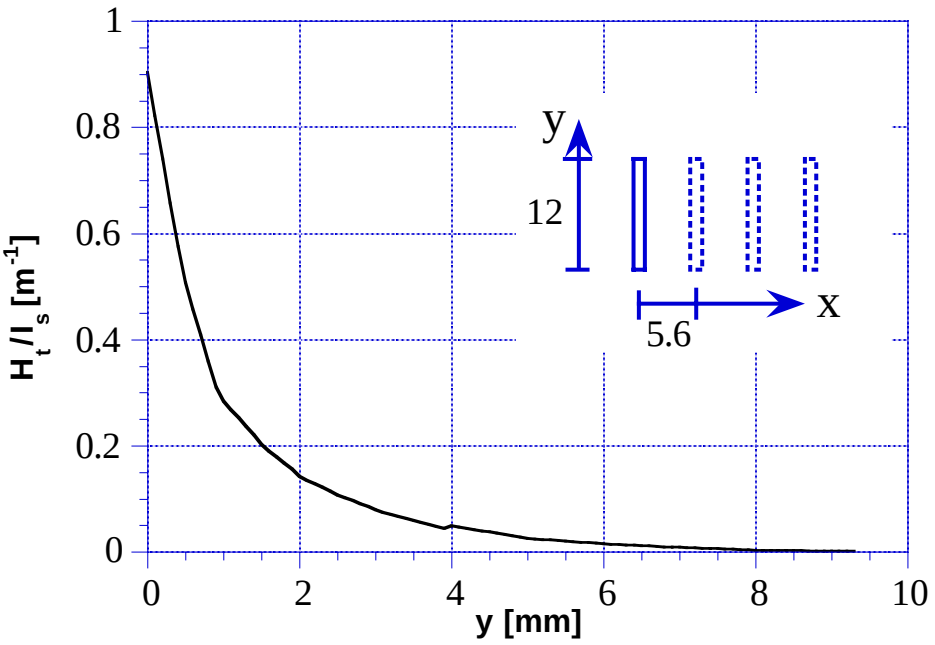

Figure 7: Field distribution along the strip contour.

Considering 5 Amps beam current, distributed over 120 bunches of 3 cm length, eq. (1) gives a Joule loss of ≈500 mW on each strip laying close to the vertical symmetry plane, while the Joule loss on the side strips is ≈100 mW. The power dissipated on the other strips is reported in the 3rd row of Table II.

3.3 Thermal analysis.

The summary of the loss estimate for the long bellows shield is reported in Table II. The strip-by-strip power dissipation is indicated for 1/4 of the structure, starting from the strip closest to the longitudinal vertical plane and ending at the wide lateral one.

Table II

Strip #	1 (central)	2	3	4	5	6	7	8 (lateral)
P_{res} [mW]	65	65	65	65	65	65	65	420
P_{Joule} [mW]	500	390	250	130	60	20	3.5	100
P_{tot} [mW]	**565**	**455**	**315**	**195**	**125**	**85**	**68.5**	**520**

A two-dimensional model has been developed to take into account the strip-to-strip thermal exchange due to the combs and the septa[5]. The data of Table II have been used as the input for a thermal simulation based on ANSYS[6], a finite element code for structural analyses.
The simulation results show that there is again a longitudinal temperature gradient, and that the hottest spot is localized in the middle of the central strips, with a temperature of ≈ 44 °C against an ambient temperature of 20 °C.

Conclusions

The various kind of losses on the DAΦNE bellows shields have been estimated and a thermal analysis has been carried out for the maximum design circulating current. The results show that the amount of heating produced by the beam image current Joule dissipation and the interception of residual synchrotron radiation is moderate and tolerable. The evaluation of the power coming from resonant coupling to the beam is much more complicate, because of the mode frequency uncertainty. Nevertheless, an estimate based on a wire measurement characterization of the long bellows shows that the resonant loss should give a contribution comparable to that coming from Joule dissipation, and therefore we are confident that in the operating regime no overheating shall occur.

References

[1] A. Gallo et al., *Impedance of DAΦNE Shielded Bellows*, Proc. of the 5th EPAC, Sitges (Barcelona), 1996, p.1371.

[2] Hewlett-Packard Co., *HFSS, The High Frequency Structure Simulator HP85180A*^{TM}.

[3] A. Clozza, private communication to the authors.

[4] R. Klatt et al., *MAFIA - A Three-Dimensional Electromagnetic CAD System for Magnets, RF Stuctures, and Transient Wake Field Calculations,* SLACreport 303, 1986.

[5] G.O. Delle Monache & G. Sensolini, *Non Sliding Contact Bellows Shield: Mechanical Design,* DAΦNE Technical Note ME-5, July 1996.

[6] ANSYS, Swanson Analysis System Inc., Houston (Pennsylvania), 15342 USA.

APPENDIX

In the following we will show how the total probability function plot in Fig. 6 has been derived.

Given a family of modes like that reported in Table I and the beam spectral structure, we have evaluated the probability that the power dissipation is lower than any given value, assuming that the mode frequencies f_k are completely uncertain, while their peak impedances Z_k (including the bunch length roll-off factor) and Q-values Q_k are known (for instance from wire measurements or code simulations). This can be a quite general approach whenever the exact resonance positions cannot be known and nevertheless it is important to estimate the system behaviour in terms of power dissipations or instability rise-times.
Let us assume that each mode of the family significantly interacts with only one beam spectrum line, so that we can define:

$$P_{M_k} = 2 Z_k I_b^2$$

$$P_{m_k} = \frac{2 Z_k I_b^2}{1 + \left(Q_k f_0 / f_k \right)^2} = \frac{P_{M_k}}{1 + \left(Q_k f_0 / f_k \right)^2} \qquad \text{(A1)}$$

where P_{M_k} and P_{m_k} are respectively the maximum and minimum power deliverable to the k-th mode, while all other symbols have been previously defined.

To get a power dissipation value P_0 between the two limit values P_{M_k} and P_{m_k}, the mode detuning Δf_0 has to be equal to:

$$\Delta f_0 = \pm \frac{f_k}{2 Q_k} \sqrt{\frac{P_{M_k}}{P_0} - 1} \qquad \text{(A2)}$$

and the power dissipated will be higher than P_0 if the detuning is inside the $\pm \Delta f_0$ range, while it will be lower than P_0 if the detuning is outside that range (but, obviously, always within the $\pm f_0 / 2$ range).

Therefore, if we define $p_k(P_0)$ as the probability that the power dissipated on the k-th mode is lower than P_0, we get:

$$p_k(P_0) = \frac{f_0 - 2\Delta f_0}{f_0} = 1 - \frac{f_k}{Q_k f_0} \sqrt{\frac{P_{M_k}}{P_0} - 1} = 1 - \sqrt{\frac{P_{M_k} / P_0 - 1}{P_{M_k} / P_{m_k} - 1}} \qquad \text{(A2)}$$

with the obvious assumption $p_k(P_0) = 0$ if $P_0 \le P_{m_k}$, and $p_k(P_0) = 1$ if $P_0 \ge P_{M_k}$.

The derivative of the $p_k(\boldsymbol{P})$ function gives the probability density:

$$\eta_k(\boldsymbol{P}) \equiv \frac{dp_k}{d\boldsymbol{P}} \tag{A3}$$

$\eta_k(\boldsymbol{P}_0)d\boldsymbol{P}$ = probability that the power dissipated is in the range$(\boldsymbol{P}_0, \boldsymbol{P}_0 + d\boldsymbol{P})$

If we consider now a population of two modes, so that the functions $p_1(\boldsymbol{P}), p_2(\boldsymbol{P}), \eta_1(\boldsymbol{P}), \eta_2(\boldsymbol{P})$ are given, the total probability density function $\eta_T(\boldsymbol{P})$ is given by:

$$\eta_T(\boldsymbol{P}_0) = \int_0^{\boldsymbol{P}_0} \eta_1(\boldsymbol{P})\ \eta_2(\boldsymbol{P}_0 - \boldsymbol{P})d\boldsymbol{P}\ = \eta_1 \otimes \eta_2\big|_{\boldsymbol{P}_0} \tag{A4}$$

where the symbol $\otimes$ designates the convolution product.

In order to extend this result to a family of N modes, it is convenient to consider the Laplace transform of the involved functions. Therefore we introduce the following notation:

$$\bar{p}_k(\boldsymbol{q}) = \mathcal{L}\left[p_k(\boldsymbol{P})\right]\ ;\ \bar{\eta}_k(\boldsymbol{q}) = \mathcal{L}\left[\eta_k(\boldsymbol{P})\right] \tag{A5}$$

Due to the properties of the Laplace transform, eq. (A4) becomes:

$$\bar{\eta}_T(\boldsymbol{q}) = \bar{\eta}_1(\boldsymbol{q}) \cdot \bar{\eta}_2(\boldsymbol{q}) \tag{A6}$$

and the extension to a population of N modes is straightforward:

$$\bar{\eta}_T(\boldsymbol{q}) = \prod_{k=1}^{N} \bar{\eta}_k(\boldsymbol{q}) \tag{A7}$$

Reminding the derivative and integral theorems, we finally obtain:

$$p_T(\boldsymbol{P}) = \mathcal{L}^{-1}\left[\bar{p}_T(\boldsymbol{q})\right] = \mathcal{L}^{-1}\left[\frac{\bar{\eta}_T(\boldsymbol{q})}{\boldsymbol{q}}\right] = \mathcal{L}^{-1}\left[\frac{1}{\boldsymbol{q}} \prod_{k=1}^{N} \bar{\eta}_k(\boldsymbol{q})\right] = \mathcal{L}^{-1}\left[\boldsymbol{q}^{N-1} \prod_{k=1}^{N} \bar{p}_k(\boldsymbol{q})\right] \tag{A8}$$

which is the expression used to compute the probability function of Fig. 6 on the basis of the modes listed in Table I.